

Construction of 3-Dimensional Printed Ultrasound Phantoms With Wall-less Vessels

Daniil I. Nikitichev, PhD, Anamaria Barburas, BSc, Kirstie McPherson, FRCA, Jean-Martial Mari, PhD, Simeon J. West, FRCA, Adrien E. Desjardins, PhD

Ultrasound phantoms are invaluable as training tools for vascular access procedures. We developed ultrasound phantoms with wall-less vessels using 3-dimensional printed chambers. Agar was used as a soft tissue-mimicking material, and the wall-less vessels were created with rods that were retracted after the agar was set. The chambers had integrated luer connectors to allow for fluid injections with clinical syringes. Several variations on this design are presented, which include branched and stenotic vessels. The results show that 3-dimensional printing can be well suited to the construction of wall-less ultrasound phantoms, with designs that can be readily customized and shared electronically.

Key Words—tissue-mimicking material; 3-dimensional printing; ultrasound phantom; vascular access; vascular ultrasound; wall-less vessels

Received June 5, 2015, from the Department of Medical Physics and Biomedical Engineering, University College London, London, England (D.I.N., A.B., J.-M.M., A.E.D.); University College Hospital, London, England (K.M., S.J.W.); and University of French Polynesia, Tahiti, French Polynesia (J.-M.M.). Revision requested June 29, 2015. Revised manuscript accepted for publication September 15, 2015.

We thank Wenfeng Xia, PhD, for helpful discussions. This work was supported by European Research Council starting grant 310970, Molecular Photoacoustic Imaging During Ultrasound-Guided Interventions, and an Engineering and Physical Research Council vacation bursary for A. Barburas.

Address correspondence to Daniil Nikitichev, PhD, Department of Medical Physics and Biomedical Engineering, University College London, Gower Street, London WC1E 6BT, England.

E-mail: d.nikitichev@ucl.ac.uk

Abbreviations
3D, 3-dimensional

doi:10.7863/ultra.15.06012

Ultrasound guidance is increasingly used to guide vascular access procedures, which include peripheral venous, central venous, and arterial cannulation. Its usefulness, however, depends considerably on the skill of the operator. Proficiency with ultrasound-guided vascular access involves extensive practice, as image interpretation and visualization of the needle tip can be challenging, and the consequences of misplacing the needle can be life threatening.^{1,2} Ultrasound phantoms are important for acquiring these clinical skills before performing on live patients; it has been shown that clinicians who undertake simulation training in ultrasound-guided vascular access achieve higher success rates.^{3,4} A wide range of commercial ultrasound phantoms have been developed for vascular access. They tend to be expensive, with lifetimes limited by the tracks created by needle insertions. As such, they are used sparingly in all but the most affluent clinical departments.

Many custom phantoms have been proposed as inexpensive alternatives to commercial phantoms.⁵ An aqueous gel such as agar can be advantageous as a tissue-mimicking material, as it can readily be remade or melted to remove needle tracks.^{6–12} Many methods for creating vessels with flow in ultrasound phantoms have been proposed, with or without vessel-mimicking materials. Vessel walls can be mimicked with tubes positioned within the tissue-mimicking material^{13–19} and more realistic geometries can be created by using 3-dimensional (3D) printing molds.^{20–23} They can be also created using tissue ex vivo^{24–29} at the expense of experimental flexibility and repeatability.

In wall-less phantoms, vessel-mimicking materials are absent; a blood-mimicking material flows through a space created in the tissue-mimicking material. These types of phantoms can be well suited to vascular access, as the vessel lumens can readily be accessed with needles, and the vessel boundaries can have realistic sonographic appearances. A simple construction method for wall-less vessels involves retracting rods positioned into a tissue-mimicking material.^{20,30–34} Wall-less vessels with more realistic geometries can be created by a lost-material method, which involves creating a solid, lumenless vessel, embedding it in a tissue-mimicking material, and subsequently melting away this vessel to create a space for the blood-mimicking material.^{21,27,35–38} Despite their advantages, wall-less phantoms are not widespread in clinical practice. Their limited adoption at present may be due in large part to the mechanical workshop skills and resources required to create chambers with ports to introduce blood-mimicking materials into the wall-vessels.

In this study, we investigated the use of 3D printing to produce ultrasound phantoms for vascular access using a wall-less design. Variations in the surface quality of the chambers, which can arise from different chamber geometries and the use of different printers, were explored.

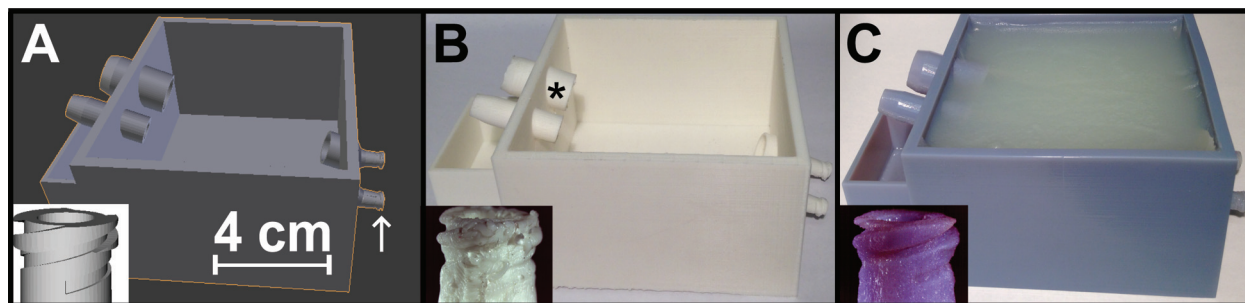
Materials and Methods

Each ultrasound phantom comprised a 3D printed rectangular chamber in which agar was poured as a soft tissue-mimicking material (Figure 1).¹⁰ The dimensions of this chamber (100 × 100 mm, 60 mm height) were compatible with typical ultrasound imaging transducers, and they allowed for in-plane and out-of-plane needle insertions. Wall-less vessels were created by placing rods in the chamber before the agar was poured and removing them after the agar was set (Figure 2, A–E). Within the chamber, the

rods were fixed in angle with small support tubes printed in the sides of the box (Figure 1). Since the diameters of the wall-less vessels were substantially larger than those of the lumens of the luer connectors, the support tubes extended out of the chamber but not within the luer connectors. On one side of the chamber, the ends of the support tubes had luer connectors that allowed for fluid to be injected through the vessels after the rods were removed (Figure 2F). Support tubes on the other side of the box could be connected to tubing (inner diameter, 8.5 mm) to receive fluid from the vessels. The support tubes protruded slightly inside the chamber to accommodate shrinkage of the agar after setting. A small tray accommodated fluid outflow when tubes on the side of the box opposite the luer connectors were not connected to tubing. Printed caps for the luer connectors were used to prevent the agar from flowing out of the chamber before it was set.

Three ultrasound phantoms with wall-less vessels were created. The first phantom comprised two parallel wall-less vessels with different diameters (12 and 6 mm) that were made by using solid rods. These diameters were chosen to correspond to a large artery/vein pair. In one variation of this phantom, the vessels were horizontal; in another, they were vertically angled at 20°. With both variations, polytetrafluoroethylene (DirectPlastics, Sheffield, England) was chosen as the material for the rods to minimize adhesion with the agar. The second phantom comprised a branched vessel, which was created with two rods. Each of these rods was 3D printed, as a combination of two hemispherical parts (Figure 3A). The first rod was positioned horizontally in the chamber, and the second was partially inserted into a groove in the first and vertically angled at 20° (Figure 3B). The 2-part rod design stemmed from the need for smooth surfaces to minimize adhesion to the agar and thereby to create smooth vessels when retracted, and from the observation that 3D printed surfaces that were

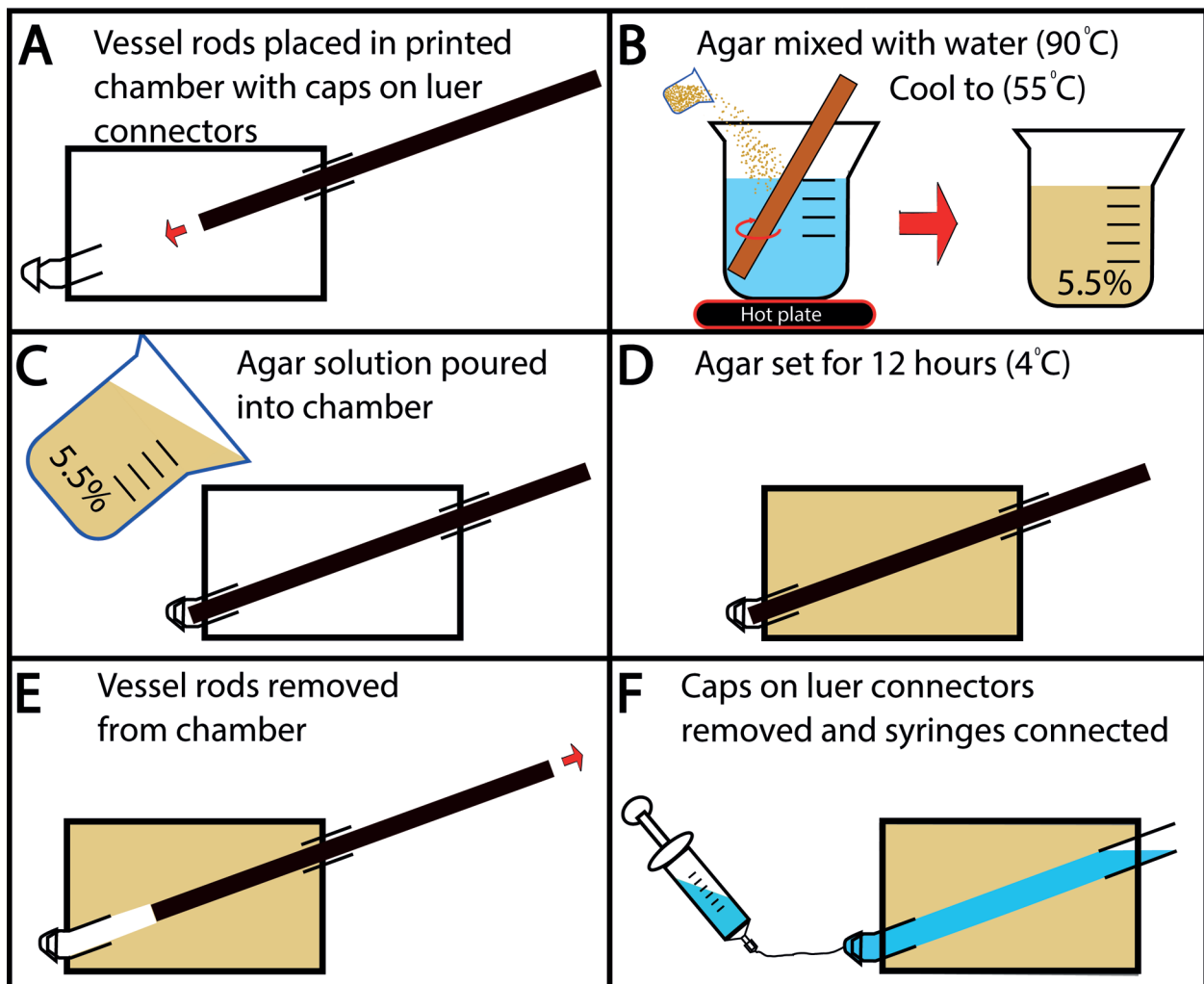
Figure 1. Chamber for a phantom with two parallel vessels: software rendering (A), output from printer 2 (B), and output from printer 1, which was filled with agar after printing (C). The insets provide close-ups of one of the luer connectors (arrow in A). Asterisk denotes support tubes.



in contact with support material during the printing process tended to be considerably less smooth than those that were not. Each hemispheric part was printed with its curved surface upward, so that it was not in contact with support material. The third phantom comprised a stenotic vessel that was created with two rods, similar to one that was previously demonstrated by Qian et al.²⁰ These rods were 3D printed in the same manner as they were for the second phantom, except that one rod had a small cavity in which the other could be positioned (Figure 3C). The diameter of these rods was 4 mm along a distance of 20 mm (centered at the point of apposition) and 6.2 mm elsewhere; the narrowing mimicked stenosis when the rods were retracted.

The chamber was designed by using two freely available software programs: Blender (Stichting Blender Foundation, Amsterdam, the Netherlands), and FreeCAD (Juergen Riegel, Werner Mayer, and Yorik van Havre; OpenSource, www.freecad.com). The 3D printing files (stereo lithography format) are included as supplemental materials. Two different printers were used; each required approximately 240 g of build material and 80 g of support material. The first printer, which will be denoted printer 1, was an additive polymer resin printer (Objet30 Pro; Stratasys, Eden Prairie, MN) using a rigid opaque white or blue material with a gloss finish (VeroWhitePlus RGD835 or VeroBlue; Stratasys). The second (printer 2) was an extruded thermo-plastic polymer printer (Ultimaker2; Ultimaker, Chorley,

Figure 2. Phantom fabrication steps using the 3D printing chamber.



England) using a filament material (PolyMax; Polymakr, Changshu, China). The printing costs for each phantom varied substantially with the printer: £44 (approximately \$64) for printer 1 and £3 (approximately \$4) for printer 2. These costs were solely for the printing materials. By comparison, the costs of commercial vascular access phantoms are typically in excess of £1000 (approximately \$1456).

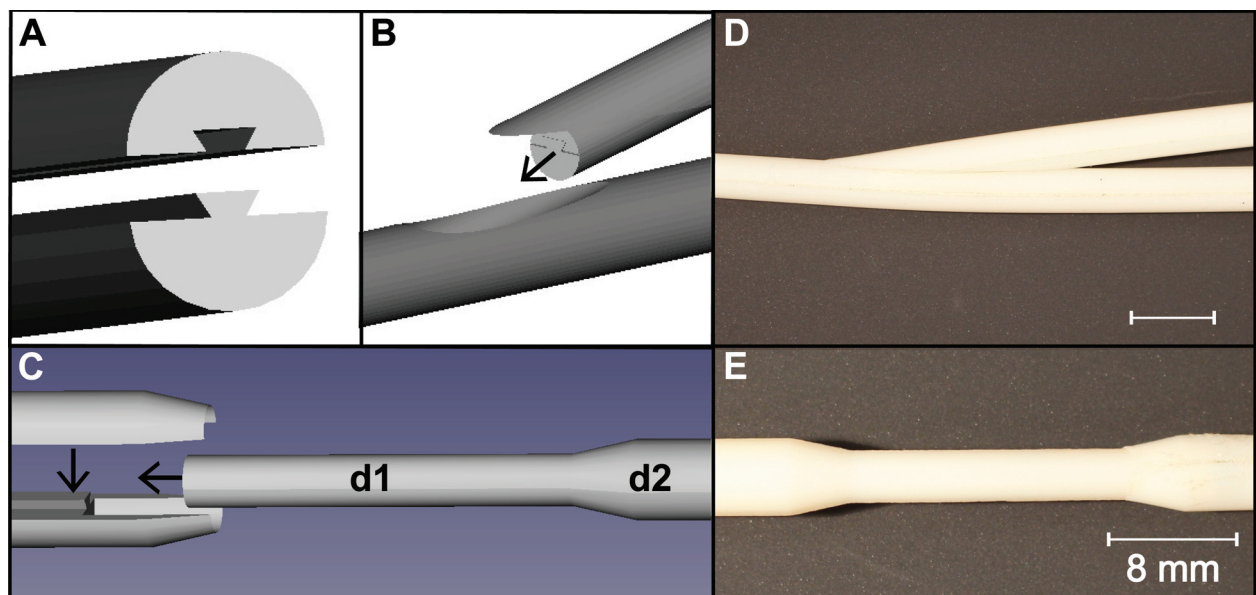
The agar (A7002; Sigma-Aldrich, St Louis, MO) was dissolved in hot water ($>90^{\circ}\text{C}$) outside the chamber to bring it above its melting point (85°C), with a concentration of 5.5% by weight. This concentration was similar to those previously used.^{16,39} A hot plate was found to be useful for maintaining the high temperature during dissolution; without it, rapid mixing would be required, and consequently there would be a risk of introducing bubbles. It was found that the use of a degassing chamber for 5 minutes was useful to remove residual bubbles.¹¹ After mixing, the melted agar solution was cooled to a temperature in the range of 50°C to 55°C , which was below the range in which the 3D printing material distorts and above the gel point of agar. The solution was poured into the 3D printed chamber, and the phantom was placed in a refrigerator (4°C) for 24 hours before the rods were removed. The cost of the agar used to create each wall-less phantom was less than £0.72 (approximately \$1.05).

The phantom was imaged with a linear array transducer (L14-5/38, SonixMDP; Analogic Ultrasound, Richmond, British Columbia, Canada). Before imaging, the vessels were filled with water using two 10-mL syringes connected directly to the chamber. In-plane and out-of-plane needle insertions were performed under ultrasound imaging guidance with an injection needle (18 gauge; Terumo Medical Corporation, Somerset, NJ).

Results

The surface quality and mechanical robustness of the 3D printed chambers depended considerably on the printing process that was used (Figure 1). Both chambers were waterproof and could withstand accidental needle pricks. Printer 1 produced a chamber with a much smoother surface, and its output had superior resolution and mechanical integrity. A prominent difference between the printer outputs was found between the luer connectors: those obtained with printer 2 readily broke with regular use, and the grooves were incompletely delineated (Figure 3, insets). Manual removal of the printing support material, which is required before the chamber can be used, could be achieved more easily when printer 1 was used.

Figure 3. Design of the vessel rods (3D drawings) for the wall-less phantom (A), the branching phantom (B), and the stenotic phantom (C); outer diameters: d1, 4 mm; d2, 6.2 mm). Printed results are shown for the branching vessel (D) and the stenotic vessel (E). Scale bars in D and E: 8 mm.

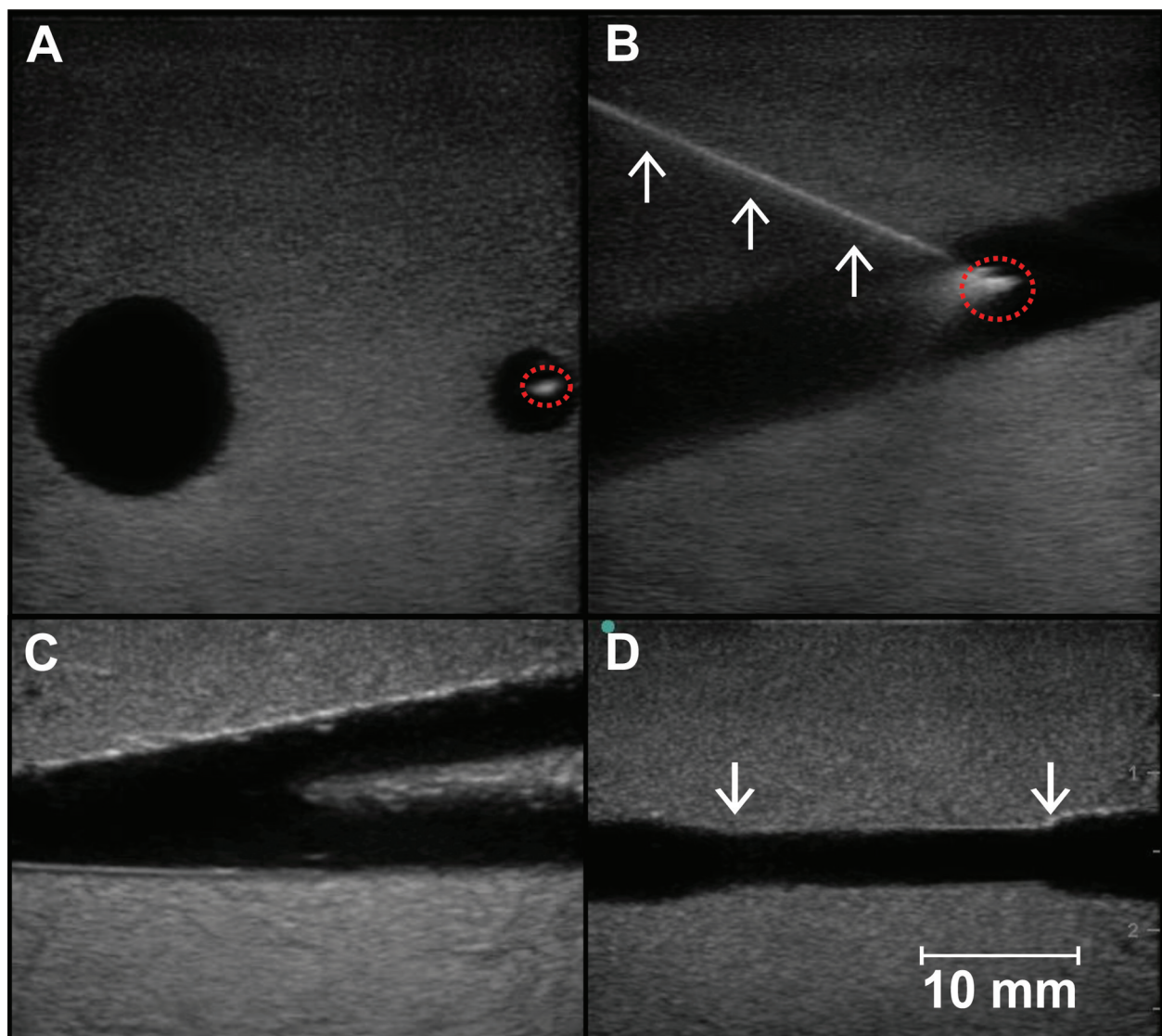


As seen on ultrasound imaging, wall-less vessels in all three phantoms had circular cross sections throughout their length (Figure 4). Needles could readily be inserted into the agar and into the vessels. The resistance to insertion was less than that typically encountered in vascular access procedures, however, and resistance was not encountered during transitions from agar to the vessel lumens. Needles were readily visualized on ultrasound imaging with out-of-plane (Figure 4A) and in-plane (Figure 4B) insertions.

Residual needle tracks were apparent, but these could be removed by remaking the phantom.

The agar surrounding these vessels had a homogeneous speckled appearance on ultrasound imaging, similar to that of tissue. At the surface of the phantoms, the agar was sufficiently rigid to resist deformation by the ultrasound transducer with light pressure consistent with clinical practice, but care was needed to ensure integrity of the surface. The vessels maintained their shape during

Figure 4. Wall-less vessel phantoms imaged with a linear array transducer. During imaging, the vessels were filled with water using two syringes connected to the chamber. Needle insertions into the parallel-vessel phantom were performed out of plane (A) and in plane (B); in the latter, the shaft is visible (arrows). The needle tip was visible in both views (dashed circles). The branching phantom (C) and the stenotic phantom (D) are imaged in cross section; in the latter, the boundaries of the narrow-diameter region are shown with arrows.



injections of water, without fluid leaks. In the branched-vessel phantom, the thin agar at the bifurcation point (Figure 4C) was prone to damage during injections. With the stenotic phantom, the variation in vessel diameter was clearly apparent (Figure 4D), and the stenotic region appeared uniform along its length, with smooth walls that tapered on either side to wider regions.

Discussion

In this study, the use of 3D printing for the manufacturing of agar wall-less vascular phantoms was explored with three different vessel geometries. The use of 3D printing has two main advantages that make it compelling for use in clinical environments. First, it makes the creation of chamber geometries with multiple-inset tubular structures and fabrication of luer connectors straightforward, even in the absence of mechanical workshop resources. Second, the design files can readily be shared electronically and modified to accommodate different types of training. The phantom chamber design lends itself to several variations that could provide different functionalities. For instance, a pump that provides pulsatile flow and blood-mimicking fluid could be used for practicing with Doppler ultrasound imaging, as considered in a previous study.^{11,20}

A homogeneous agar region surrounding the wall-less vessels is attractive from the standpoint of simplicity, but the use of different materials could allow for inhomogeneities that increase realism. As a variation on the phantom in this study, different layers of aqueous gels could be formed by pouring melted gel on top of a set gel layer; the resulting layers could have additions with different concentrations to control their sonographic properties. For instance, gelatin, as an aqueous gel, could include a combination of graphite particles for control of ultrasound attenuation and alcohol for control of the speed of sound.^{10,12} Ultimately, 3D printing could be used to deposit soft tissue-mimicking materials directly with 3D printing, which could lead to printing complex structures such as the brachial plexus and even to creating patient-specific phantoms based on segmented preprocedural images. An analogous approach was explored for creating optical phantoms.⁴⁰

One limitation of wall-less vessel phantoms created to date has been their fragility. Some of these phantoms rupture when used under physiologic flow conditions, particularly when a high degree of stenosis is present in the phantom.^{37,38} The fragility of tissue-mimicking materials might be greatly reduced with the use of tissue-mimicking materials that are more mechanically robust than those based on aqueous gels, such as polyvinyl chloride-plastisol.⁴¹

Nonetheless, a vessel-mimicking material may be better suited to certain applications than a wall-less vessel: for instance, when realistic mechanical properties of arteries are required.⁸

This study demonstrated that 3D printing is well suited to the creation of wall-less vascular ultrasound phantoms that include branched and stenotic vessels. The approach taken in this study is particularly well suited to efficient, low-cost vascular phantoms for clinical training.

References

1. Blaivas M, Adhikari S. An unseen danger: frequency of posterior vessel wall penetration by needles during attempts to place internal jugular vein central catheters using ultrasound guidance. *Crit Care Med* 2009; 37: 2345–2349.
2. Bohlega S, Mclean DR. Hemiplegia caused by inadvertent intra-carotid infusion of total parenteral nutrition. *Clin Neurol Neurosurg* 1997; 99:217–219.
3. McGaghie WC, Issenberg SB, Petrusa ER, Scalese RJ. A critical review of simulation-based medical education research: 2003–2009. *Med Educ* 2010; 44:50–63.
4. Evans LV, Dodge KL, Shah TD, et al. Simulation training in central venous catheter insertion: improved performance in clinical practice. *Acad Med* 2010; 85:1462–1469.
5. Hocking G, Hebard S, Mitchell CH. A Review of the benefits and pitfalls of phantoms in ultrasound-guided regional anesthesia. *Reg Anesth Pain Med* 2011; 36:162–170.
6. Lo MD, Ackley SH, Solari P. Homemade ultrasound phantom for teaching identification of superficial soft tissue abscess. *Emerg Med J* 2012; 29:738–741.
7. Poepping TL, Nikolov HN, Thome ML, Holdsworth DW. A thin-walled carotid vessel phantom for Doppler ultrasound flow studies. *Ultrasound Med Biol* 2004; 30:1067–1078.
8. King DM, Ring M, Moran CM, Browne JE. Development of a range of anatomically realistic renal artery flow phantoms. *Ultrasound Med Biol* 2010; 36:1135–1144.
9. Surry KJM, Austin HJB, Fenster A, Peters TM. Poly(vinyl alcohol) cryogel phantoms for use in ultrasound and MR imaging. *Phys Med Biol* 2004; 49:5529–5546.
10. Madsen EL, Zagrebski JA, Banjavie RA, Jutila RE. Tissue-mimicking materials for ultrasound phantoms. *Med Phys* 1978; 5:391–394.
11. Lai SSM, Yiu BYS, Poon AKK, Yu ACH. Design of anthropomorphic flow phantoms based on rapid prototyping of compliant vessel geometries. *Ultrasound Med Biol* 2013; 39:1654–1664.
12. Culjat MO, Goldenberg D, Tewari P, Singh RS. A review of tissue substitutes for ultrasound imaging. *Ultrasound Med Biol* 2010; 36:861–873.
13. Teirlinck CJPM, Bezemer RA, Kollmann C, et al. Development of an example flow test object and comparison of five of these test objects, constructed in various laboratories. *Ultrasonics* 1998; 36:653–660.

14. Di Domenico S, Santori G, Porcile E, Licausi M, Centanaro M, Valente U. Inexpensive homemade models for ultrasound-guided vein cannulation training. *J Clin Anesth* 2007; 19:491–496.
15. Kendall JL, Faragher JP. Ultrasound-guided central venous access: a homemade phantom for simulation. *Can J Emerg Med* 2007; 9:371–373.
16. Chantler J, Gale L, Weldon O. A reusable ultrasound phantom. *Anaesthesia* 2004; 59:1145–1146.
17. Dineley J, Meagher S, Poepping TL, McDicken WN, Hoskins PR. Design and characterisation of a wall motion phantom. *Ultrasound Med Biol* 2006; 32:1349–1357.
18. Embree PM, O'Brien WR. Volumetric blood flow via time-domain correlation: experimental verification. *IEEE Trans Ultrason Ferroelectr Freq Control* 1990; 37:176–189.
19. Morrow DS, Broder J. Cost-effective, reusable, leak-resistant ultrasound-guided vascular access trainer. *J Emerg Med* 2015; 49:313–317.
20. Qian M, Song R, Niu L, Chen L, Zheng H. Two-dimensional flow study in a stenotic artery phantom using ultrasonic particle image velocimetry. *Conf Proc IEEE Eng Med Biol Soc* 2011; 2011:563–566.
21. Watts DM, Sutcliffe CJ, Morgan RH, et al. Anatomical flow phantoms of the nonplanar carotid bifurcation, part I: computer-aided design and fabrication. *Ultrasound Med Biol* 2007; 33:296–302.
22. Yedavalli RV, Loth F, Yardimci A, et al. Construction of a physical model of the human carotid artery based upon in vivo magnetic resonance images. *J Biomech Eng* 2001; 123:372–376.
23. O'Flynn PM, Roche ET, Pandit AS. Generating an ex vivo vascular model. *ASAIO J* 2005; 51:426–433.
24. Greaby R, Zderic V, Vaezy S. Pulsatile flow phantom for ultrasound image-guided HIFU treatment of vascular injuries. *Ultrasound Med Biol* 2007; 33:1269–1276.
25. Dabrowski W, Dunmore-Buyze J, Rankin RN, Holdsworth DW, Fenster A. A real vessel phantom for imaging experimentation. *Med Phys* 1997; 24:687–693.
26. Dabrowski W, Dunmore-Buyze J, Cardinal HN, Fenster A. A real vessel phantom for flow imaging: 3-D Doppler ultrasound of steady flow. *Ultrasound Med Biol* 2001; 27:135–141.
27. Bale-Glickman J, Selby K, Saloner D, Savaş O. Experimental flow studies in exact-replica phantoms of atherosclerotic carotid bifurcations under steady input conditions. *J Biomech Eng* 2003; 125:38–48.
28. Kerber CW, Heilman CB. Flow dynamics in the human carotid artery, I: preliminary observations using a transparent elastic model. *AJNR Am J Neuroradiol* 1992; 13:173–180.
29. Motomiya M, Karino T. Flow patterns in the human carotid artery bifurcation. *Stroke* 1984; 15:50–56.
30. Guo Z, Fenster A. Three-dimensional power Doppler imaging: a phantom to quantify vessel stenosis. *Ultrasound Med Biol* 1996; 22:1059–1069.
31. Cloutier G, Soulez G, Qanadli SD, et al. A multimodality vascular imaging phantom with fiducial markers visible in DSA, CTA, MRA, and ultrasound. *Med Phys* 2004; 31:1424–1433.
32. Kenwright DA, Laverick N, Anderson T, Moran CM, Hoskins PR. Wall-less flow phantom for high-frequency ultrasound applications. *Ultrasound Med Biol* 2015; 41:890–897.
33. Ramnarine KV, Anderson T, Hoskins PR. Construction and geometric stability of physiological flow rate wall-less stenosis phantoms. *Ultrasound Med Biol* 2001; 27:245–250.
34. Qian M, Niu L, Wong KKL, Abbott D, Zhou Q, Zheng H. Pulsatile flow characterization in a vessel phantom with elastic wall using ultrasonic particle image velocimetry technique: the impact of vessel stiffness on flow dynamics. *IEEE Trans Biomed Eng* 2014; 61:2444–2450.
35. Frayne R, Gowman LM, Rickey DW, et al. A geometrically accurate vascular phantom for comparative studies of x-ray, ultrasound, and magnetic resonance vascular imaging: construction and geometrical verification. *Med Phys* 1993; 20:415–425.
36. Poepping TL, Nikolov HN, Rankin RN, Lee M, Holdsworth DW. An in vitro system for Doppler ultrasound flow studies in the stenosed carotid artery bifurcation. *Ultrasound Med Biol* 2002; 28:495–506.
37. King DM, Moran CM, McNamara JD, Fagan AJ, Browne JE. Development of a vessel-mimicking material for use in anatomically realistic Doppler flow phantoms. *Ultrasound Med Biol* 2011; 37:813–826.
38. Meagher S, Poepping TL, Ramnarine KV, Black RA, Hoskins PR. Anatomical flow phantoms of the nonplanar carotid bifurcation, part II: experimental validation with Doppler ultrasound. *Ultrasound Med Biol* 2007; 33:303–310.
39. West SJ, Mari JM, Khan A, et al. Development of an ultrasound phantom for spinal injections with 3-dimensional printing. *Reg Anesth Pain Med* 2014; 39:429–433.
40. Wang J, Coburn J, Liang CP, et al. Characterization and application of 3D-printed phantoms for biophotonic imaging. *Proc SPIE* 2013; 8719:87190Y.
41. Spirou GM, Oraevsky AA, Vitkin IA, Whelan WM. Optical and acoustic properties at 1064 nm of polyvinyl chloride-plastisol for use as a tissue phantom in biomedical optoacoustics. *Phys Med Biol* 2005; 50:N141–N153.